Polymer 50 (2009) 3786–3796

Contents lists available at ScienceDirect

Polymer

journal homepage: www.elsevier.com/locate/polymer

Role of polymer–clay interactions and nano-clay dispersion on the viscoelastic response of supercritical CO_2 dispersed polyvinylmethylether (PVME)–Clay nanocomposites

Mihai Manitiu, Steven Horsch [1], Esin Gulari [2], Rangaramanujam M. Kannan*

Wayne State University, Chemical Engineering and Materials Science, Detroit, MI 48202, USA

ARTICLE INFO

Article history:
Received 1 April 2009
Received in revised form
11 May 2009
Accepted 19 May 2009
Available online 27 May 2009

Keywords:
Supercritical CO_2 processing
Dispersed polymer–clay nanocomposites
Rheology

ABSTRACT

Clay dispersion and polymer–clay interactions play a key role in producing property enhancements in nanocomposites; yet characterizing them in complex polymer–clay systems is often a challenge. Rheology can offer insights into clay dispersion and clay–polymer interactions. We have investigated the viscoelastic response for a series of supercritical CO_2 ($scCO_2$) processed polyvinylmethylether (PVME)/clay nanocomposites with varying polymer–clay interactions and nano-clay dispersion. PVME is used in this study because it is highly swellable in $scCO_2$, thereby enabling processing of PVME/clay mixtures without the presence of a co-solvent. Since PVME and natural clay are water-soluble, highly dispersed PVME-clay nanocomposites were prepared using water, followed by lyophilization in the presence of polymer. In this 'weakly interacting', but highly dispersed systems, with clay loadings above the percolation threshold, terminal behavior was observed in the linear viscoelastic moduli (i.e. no low frequency plateau is observed). When the nanocomposites were processed in $scCO_2$, with 15 wt% of 30B and I.30P, the WAXD patterns of the resultant nanocomposites were largely comparable, indicating partial dispersion, with intercalation peaks. However, the rheology of these two nanocomposites were significantly different despite similar inorganic volume loading (4 vol%). Even with less dispersion compared to the water-based system, the low-frequency moduli were significantly more enhanced, accompanied by a plateau, and a cross-over frequency shift. Neglecting the small differences in the actual clay content between these clays (4–5 vol% of inorganic matter), this suggests that rheology may be sensitive to strong interactions between the clay surfactant and the polymer. Therefore, polymer–clay interactions and clay–clay interactions may both be important in the ability to sustain a "so-called" percolated network, rather than just clay dispersion.

1. Introduction

Polymer nanocomposites comprised of highly anisotropic layered silicates have attracted considerable attention because of their potential to lead to materials with exceptional thermal, barrier, and mechanical properties. A key to several of the improvements is exfoliation/intercalation of the nano-clay to expose the large available surface area to the host matrix and increase the effective aspect ratio of the nano-clay particles [1–11]. Typically, the first step in producing montmorillonite based nanocomposites is subjecting the nano-clay to an ion-exchange reaction to expand the inter-gallery spacing and render the clay organophilic [12]. The organophilic nano-clay can then be melt processed, *in situ* polymerized, or solution cast to produce nanocomposites with varying degrees of dispersion ranging from intercalated to exfoliated [13–22].

Over the past decade, considerable effort has been put forth to understand the structure–property relationships of polymer/clay nanocomposites. In particular, the linear viscoelastic response of polymer–clay nanocomposites has been extensively studied in order to understand the mechanical and rheological properties of these systems and elucidate how these properties relate to the type of microstructure/mesostructure formed [22–26]. In general, these investigations revealed that the principle of time–temperature superposition is obeyed with the temperature dependence of the frequency shift factor (a_T) being independent of silicate loading and dispersion. Moreover, the mesoscale dispersion strongly impacts

* Corresponding author. Wayne State University, Chemical Engineering and Materials Science, 1121 Engineering, 5050 Anthony Wayne Drive, Detroit, MI 48202, USA. Tel.: +313 577 3879; fax: +313 577 3810 .
E-mail address: rkannan@eng.wayne.edu (R.M. Kannan).
[1] Currently at Dow Chemical, Freeport, TX.
[2] Currently at Clemson University.

0032-3861/$ – see front matter © 2009 Elsevier Ltd. All rights reserved.
doi:10.1016/j.polymer.2009.05.036

the low frequency viscoelastic behavior of the dynamic moduli and the low shear rate viscosity. Good dispersion typically results in a low frequency plateau in the storage modulus (G′) and diverging complex viscosity at low shear rates. The pseudo solid-like behavior has been attributed to a "so-called" percolated structure [27]. However, as Krishnamoorti and Giannelis demonstrated for example, a sufficient active interaction between the polymer (soft phase) and the clay (hard phase) is a necessary component for pseudo solid-like rheological behavior to be prevalent [24]. In some of their nanocomposites, the matrix polymers utilized were only lightly entangled yet a low frequency plateau was observed in G′ suggesting that entanglement is not a necessity for pseudo solid-like behavior to exist. We have recently reported the rheological response of dispersed PDMS/clay and PS/clay nanocomposites prepared by a novel supercritical CO_2 ($scCO_2$) processing method. In these nanocomposites the pseudo solid-like low frequency response appeared dependent on the "effective" molecular weight of the polymer [28,29]. Our results suggest that low molecular weight polymer chains may preferentially transport to the nano-clay surface because of their increased solubility in $scCO_2$. As a result, the polymer chains interacting with the nano-clay surface are too short to form a network with the bulk polymer or other clay structures and liquid-like behavior is observed even when the nano-clay is highly dispersed. We have also seen pseudo solid-like behavior in PS based nanocomposites that have good interactions between the PS matrix and the nano-clay surface [30]. In the case of the PS based nanocomposites the molecular weight of the polymer was 5000 g/mol, well below the entanglement molecular weight of PS, and as such the chains were not capable of forming a network between chains on the clay surface and the host matrix. Therefore, it appears that in the absence of good interactions, high molecular weight polymers may still be able to help sustain the mesoscale structure. In cases where good polymer–clay interactions exist, entanglement between chains on the clay surface and in the bulk may not be a necessary component to sustain the structure.

In this study, we investigate the role of polymer–clay interactions and filler dispersion on the linear viscoelastic response of *$scCO_2$ processed* polymer clay nanocomposites. Polyvinylmethylether (PVME) was chosen as the host matrix for natural montmorillonite and three organophilic nano-clays. PVME appears to be highly swellable in $scCO_2$ even at a molecular weight of 90,000 g/mol. In contrast to other $scCO_2$-swellable polymers, such as PDMS and PS, PVME is hydrophilic, and may enable processing of even natural clay. Natural montmorillonite was chosen as a reference for the strength of the polymer–filler interactions because it has weak interactions with PVME. Poly(ethylene oxide) (PEO) was also used as the host matrix for natural montmorillonite to compare the extent of PEO-filler interactions with that of PVME-filler interaction. In contrast, the organophilic clays used in this study may have varying degrees of interaction with the host matrix, in addition to having different clay dispersions upon $scCO_2$ processing. Specifically, Cloisite 30B (methyl tallow bis-2-hydroxyethyl ammonium salt) may form a hydrogen bond between the host matrix and the surfactant, and Nanomer I.30P (trimethyl hydrogenated tallow ammonium salt) has a moderate loading of alkyl groups, thereby altering the extent of the polymer–clay interactions in each system. The *$scCO_2$ processed* nanocomposites were contrasted with a highly dispersed (disordered) Cloisite Na^+/PVME nanocomposite produced from a solution cast/freeze drying method, with water as a solvent. As a result of the selected processing conditions, the nanocomposites produced via the *$scCO_2$ method* had intercalated or disordered intercalated morphologies.

The rheological response of the partially exfoliated Cloisite Na^+/PVME nanocomposite is compared with the response of the intercalated Cloisite Na^+/PVME nanocomposite to understand the role of clay structure on the linear viscoelasticity of "weakly-interacting" polymer/clay nanocomposites. The rheological response of Cloisite Na^+/PEO was compared to that of Cloisite Na^+/PVME to understand the role of polymer–clay interactions in the two nanocomposites and demonstrate that in the case of PVME/Na^+ system there are weak interactions present. And, the viscoelastic response of intercalated organophilic clay–PVME nanocomposites is compared to the intercalated "weakly-interacting system" to determine the impact of specific polymer–clay interactions. The molecular weight of the polydispersed PVME used in this study is 90,000 g/mol, which has ~13 entanglements per chain and should be of sufficient chain length to create a network between polymer chains near the clay surface, the bulk polymer, and the mesoscale structure (PVME has an entanglement molecular weight of 6450 g/mol [31]). In addition, all the nanocomposites had a nano-clay loading of 15 wt% to ensure that a percolated structure could form even if the nanocomposites were intercalated. The existence of a "so-called" percolated structure allows us to probe the role of polymer–clay interactions on the ability to sustain this nano-clay network under deformation.

2. Experimental methods

2.1. Materials

The Cloisite series of clays 30B and Na^+ used in this study were obtained from Southern Clay Products and the I.30P was provided by Nanocor. The composition and physical properties of the clays are summarized in Table 1. The PVME used in this research was purchased from Scientific Polymer Product Inc. The polydispersed PVME used had a weight average molecular weight of 90,000 g/mol (density of 1.05 g/ml at 20 °C) and was shipped in water. Before nanocomposite preparation, the PVME was cooled to −25 °C and placed in a freeze dryer for 4 days to remove the water. The polymer was then dissolved in toluene and filtered to remove any impurities. The toluene was removed in a vacuum oven operated at 80 °C for 2 weeks. The PEO used in this study had a molecular weight of 100,000 g/mol and was purchased from Scientific Polymer Product Inc.

2.2. $scCO_2$ Processing

The $scCO_2$ processing method exposes the polymer nano-clay mixtures to CO_2 in a high pressure vessel; the system is then raised above the critical point for CO_2 and the material is allowed to soak for an appropriate time; the system is then rapidly depressurized to atmospheric pressure. A preliminary hypothesis for the mechanism is: during the soak step, under the selected processing conditions, the mixture of the CO_2 and polymer diffuses between the clay layers. The high diffusivity and low viscosity of the CO_2-philic polymer in the mixture enable clay layer penetration. During depressurization, expansion of the $scCO_2$ between the layers pushes them apart resulting in delaminated or intercalated nanocomposites. When the CO_2 is completely removed the organic material remains between the layers, coating the surfaces of the layers, exposing the host matrix to the large available surface area of the nano-clays [28–30,32–35].

2.3. Nanocomposite formation via $scCO_2$ processing

Three PVME/clay nanocomposites were formed via $scCO_2$ processing: 15 wt% Cloisite Na^+ (15-NA), 15 wt% Cloisite 30B (15-30B), and 15 wt% I.30P (15-I.30P). Also, a 15 wt% Cloisite Na^+/PEO nanocomposite was processed via $scCO_2$ processing. The nanocomposites were formed by mechanically mixing the nano-clay

Table 1
Nano-clay surfactant composition, basal spacing, and platelet density, as reported by supplier. T is Tallow (~65% C18; ~30% C16; ~5% C14) and HT-Hydrogenated Tallow (~65 wt% C18; ~30 wt% C16; ~5 wt% C14).

Nanoclay name	Organic modifier	d_{001} spacing (nm)	Density (g/ml)
Cloisite Na^+	None	1.2	2.86
Cloisite 30B	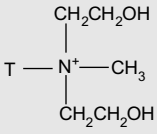	1.85	1.98
I.30P	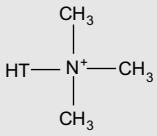	2.3	1.71

with PVME or PEO and then processing the mixture in $scCO_2$, under quiescent conditions, for 24 h at a temperature of 75 °C and a pressure of 13.78 MPa. The system was then rapidly depressurized to atmospheric pressure. The high loadings of nano-clay were to insure a percolated structure was possible even if the nanocomposite was intercalated rather than exfoliated.

2.4. Nanocomposite formation via solution cast freeze drying

A natural montmorillonite/PVME nanocomposite (15NA-S) was formed by mixing 1 g of Cloisite Na^+ with 500 ml of distilled water in a sealed container. The mixture of clay and *water* were vigorously mixed for 96 h at which time 5.7 g of PVME was added. The mixture was stirred for an additional 48 h, rapidly frozen with liquid nitrogen and kept in a freezer at −30 °C for 12 h. The frozen mixture was placed in a freeze dryer for 14 days to remove the water. Immobilizing the exfoliated nano-clay platelets in a polymer matrix via freezing the mixture prevented the nano-clay platelets from reorganizing into tactoids during the removal of the solvent.

2.5. Wide-angle X-ray diffraction (WAXD)

WAXD was used to determine the inter-gallery spacing of the neat clay and the clay in the polymer–clay nanocomposites. The d_{001} spacing was determined using the JADE software accompanying the diffractometer. The inter-gallery spacing was calculated by subtracting 1 nm (platelet thickness) from the d_{001} spacing. All data were collected using a Rigaku Rotaflex Powder Diffractometer with a CuKα X-ray source ($\lambda = 1.54$ Å) and an accelerating voltage of 40 kV at a current of 150 mA. To perform scans, samples were placed in a custom made zero background quartz sample-holder that is 0.9 mm in depth. Diffraction data was collected from 1 to 10° 2 theta at a step size of 0.03° and at a rate of 0.3 °/min. XRD was collected before and after performing melt rheological measurements to assure that that no changes are taking place during rheological measurements.

2.6. Rheology

Melt rheological measurements were performed under oscillatory shear using an RSA II rheometer (shear sandwich geometry 15.98 × 12.7 × 0.55 mm^3). Measurements were carried out at temperatures of 30, 55, and 80 °C for PVME and 80 °C and 100 °C for PEO; and the data were time–temperature superimposed by using a frequency shift factor (a_T). The experimental shear frequency range was $0.01 \leq \omega \leq 100$ rad s^{-1} for all samples. The samples were loaded, compressed and allowed to equilibrate for 1 h at the desired temperature. Linear viscoelastic measurements were made at low strains ($\gamma_o < 0.07$) and strain sweeps were performed to ensure the dynamic moduli were independent of the strains utilized. Each set of rheological measurements took about 10 h and after the first set was completed a second set of measurements were carried out the following day to check results reproducibility.

2.7. Thermogravimetric analysis (TGA)

TGA of the nanocomposites was performed on a Perkin–Elmer Pyris 1 instrument. Measurements were done in a nitrogen atmosphere and at a heating rate of 10 °C min^{-1} over a temperature range of 50 °C–550 °C. The sample was loaded at 20 °C and raised to 50 °C over a period of 10 min. The sample was allowed to equilibrate for an additional 10 min at 50 °C prior to starting the temperature ramp test.

3. Results and discussion

3.1. Determination of clay mass fraction in organophilic nano-clays

The organophilic nano-clays consist of platelets and organically modified ammonium salts. In determining the percolation threshold for the nano-clay it is necessary to know the mass fraction of clay because only the clay plays a role in the creating the percolated network. In order to determine the mass fraction for a particular nano-clay, TGA analysis was performed. Analysis was performed on all the organophilic nano-clays and sodium montmorillonite. The natural clay was tested to ensure that the clay itself did not decompose and skew the results of the TGA analysis. Further, the testing was performed in the absence of polymer to guarantee that the weight loss was only due to the ammonium salt modifier on the clay surface. Cloisite Na^+, 30B, and Nanocor I.30P retained 94%, 76% and 69% of their total mass respectively (Fig. 1). The actual loading of clay in 15–30B, and 15-I.30P samples is 11.4 wt%, 10.35 wt% respectively, and the loading for samples 15-NA and 15NA-S is 14.1 wt%. The 6% reduction in weight of the Cloisite Na^+ was attributed to evaporation of water and the weight losses in the organophilic clays was attributed entirely to loss of organic modifier. The actual weight fraction of clay ranged from 10.35 to 14.1 wt%, which is still well above the theoretical reported value of 4–7 wt% (1.4–2.7 vol% – depending on the clay used and its density) needed for percolation to occur [27]. Assuming that the inorganic clay layers have the density of the unmodified nano-clay matter

(2.86 g/cm^3 for Cloisite series and 2.6 g/cm^3 for) both Cloisite 30B and Nanocor I.30P nanocomposites contain 4 vol% of inorganic matter. Cloisite Na^+ nanocomposites contain 5 vol% of inorganic matter. The percolation threshold depends on the morphology of the clay (aggregates, self-assembly, interlaced, exfoliated, or any combination of these) and it can occur above or below the theoretical value. However, in our system we are well above the theoretical threshold and we believe that it is reasonable to assume that the nano-clays have formed a "so-called" percolated network.

3.2. Role of substantial nano-clay dispersion with 'weak' polymer–clay interactions

In this section, we explore the role of *substantial* nano-clay dispersion on the linear viscoelastic response in systems where only "weak polymer–clay interactions" are present. In order to achieve this goal we have prepared two PVME/Cloisite Na^+ nanocomposites. In one of the samples Cloisite Na^+ was *intercalated* with PVME via *scCO$_2$ processing* (sample 15-NA) and the other was highly dispersed in PVME via a solution cast freeze drying method using water as a solvent (sample 15NA-S). The nano-clay, Cloisite Na^+, was chosen for two reasons: (1) it swells and disperses in water (the use of a high concentration water–PVME–clay solution, and the subsequent freeze drying is expected to largely prevent clay-reaggregation), and (2) there are no oligomeric modifiers to form solvent/solute interactions, hydrogen bonds, or any other specific interaction with the host PVME. Therefore, these two samples are used to clarify the role of dispersion on the linear viscoelasticity of *"weakly interacting"* polymer clay systems as well as providing a reference point for the polymer–filler interaction. Also, we have prepared an *intercalated* Cloisite Na^+/PEO nanocomposite using $scCO_2$ technique to attempt to compare the extent of polymer/clay interactions in the $scCO_2$ processed Cloisite Na^+/PVME.

3.2.1. PVME versus PEO

WAXD was used to determine the nano-clay morphology in the host PVME and PEO polymer (Fig. 2). In contrast to the organophilic clays (to be discussed later in Section 3.1) the Cloisite Na^+/PVME sample (15-NA) displayed a low intensity, poorly-defined d_{001} diffraction peak and an absence of higher order peaks. Tactoid size could not be determined for this sample using the Scherrer equation because the diffraction peak did not resemble a Gaussian distribution and the intensity was too low. The diffraction patterned for this nanocomposite was collected again at a slower rate 0.1°/min in an attempt to obtain a better peak, but no significant changes in the diffraction pattern were observed. One possible explanation for the low intensity peak is that the inter-gallery spacing of the Cloisite Na^+ in sample 15-NA achieved a similar equilibrium spacing as the organo-philic nano-clays resulting in weak parallel registry of the clay platelets. If the platelets are not parallel and one side/end is more open than the opposite, the inter-gallery spacing (d_{001}) couldn't be determined since the spacing varies from one end to the other and WAXD is not sensitive to this morphology. This expansion correlates to more than an order of magnitude increase in the inter-gallery spacing of Cloisite Na^+ ($\sim$0.2 nm to $\sim$2.6 nm). Since the clay platelets are held together by van der Waals forces, Lennard – Jones potential is often used to model such forces and the attractive force scales inversely with the distance between attractive particles to the 6th power [17]. Therefore, the attractive forces decrease exponentially as the platelet distance increases. Further, in the case of Cloisite Na^+, there are no oligomeric modifiers on the surface that can assist in stabilizing the parallel registry of the platelets at large distances.

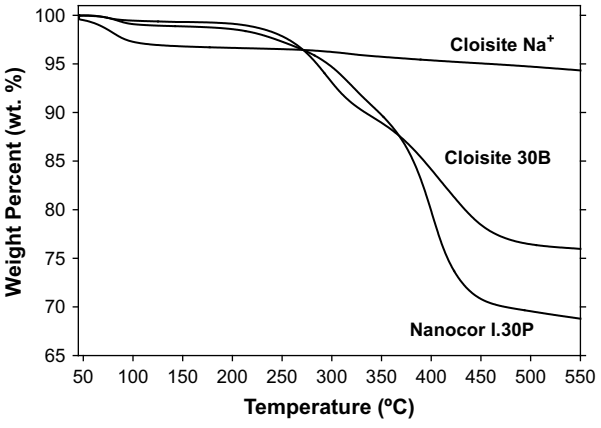

Fig. 1. TGA analysis of pure nano-clays, Cloisite Na^+, Cloisite 30B and Nanocor I.30P. The 6% reduction in weight of Cloisite Na^+ is attributed to the evaporation of water. Cloisite 30B organophilic nano-clay contains 14 wt% ammonium salt. Nanocor I.30P organophilic nano-clay contains 31 wt% ammonium salt.

A distinctive difference between the $scCO_2$ processed Na^+/PEO nanocomposite and the $scCO_2$ processed Na^+/PVME nanocomposite is the smaller final inter-gallery spacing of 1.9 nm for the PEO sample compared to 2.6 nm for the PVME sample (15-NA). Although, both $scCO_2$ nanocomposites are intercalated, the smaller final spacing may indicate that a smaller amount of polymer may have penetrated the inter-gallery spacing of the Cloisite Na^+/PEO nanocomposite. There might be some polymer that has been intercalated in interstitial spacing of the clay layers; however this could be the possibility in all the nanocomposites and we believe that it does not play a big role in our results.

Despite showing a much smaller final inter-gallery spacing compared to 15 wt% Cloisite Na^+/PVME nanocomposite, the 15 wt% Cloisite Na^+/PEO nanocomposite shows an approximately 2500% improvement in G′ at low frequencies over pure PEO along with a low frequency plateau (Fig. 3f). In contrast, the Cloisite Na^+/PVME only shows a 100% improvement in G′ at low frequencies and does not display a low frequency plateau in the frequency range tested. Since the extent of dispersion is higher in the Cloisite Na^+/PVME nanocomposite (based on WAXD), the lack of a substantial improvement in the low-frequency moduli (compared to PEO system), suggests that the extent of interactions between Cloisite Na^+ and PVME is 'weak', at least relative to that of PEO. Furthermore, the intercalated Cloisite Na^+/PEO nanocomposite shows 'comparable' improvements in G′ at low frequencies compared with the "highly dispersed" 15-NA-S sample, further supporting the claim that the level of interactions between PEO and Cloisite Na^+ are stronger than in the case of PVME and Na^+. Pandey and Farmer showed that in the presence of repulsive polymer matrix clay layers exfoliate and in the presence of attractive polymer matrix, clay platelets intercalate [36]. Their findings further support our WAXD and rheological observations. Strawhecker and Manias indicated that there are strong specific interactions between the ether oxygens and the sodium interlayer cations between PEO and Cloisite Na^+ [37]. PVME is a water-soluble polymer, with a sub-ambient glass transitions temperatures and very similar solubility parameters like PEO with one ether linkage per repeating unit. While PVME is unable to crystallize as PEO can, these polymers are otherwise quite similar. Therefore, it is expected that PVME will have some interaction with the sodium ions present in-between the layers of Cloisite Na^+. However, in Na^+/PVME sample these interactions are very weak compared to Na^+/PEO sample as evident from the significant differences in the rheological behavior between the two nanocomposites (Fig. 3e and f), despite a larger inter-gallery spacing in the PVME nanocomposite compared to the PEO sample (Fig. 2). Therefore, we will refer to the Cloisite

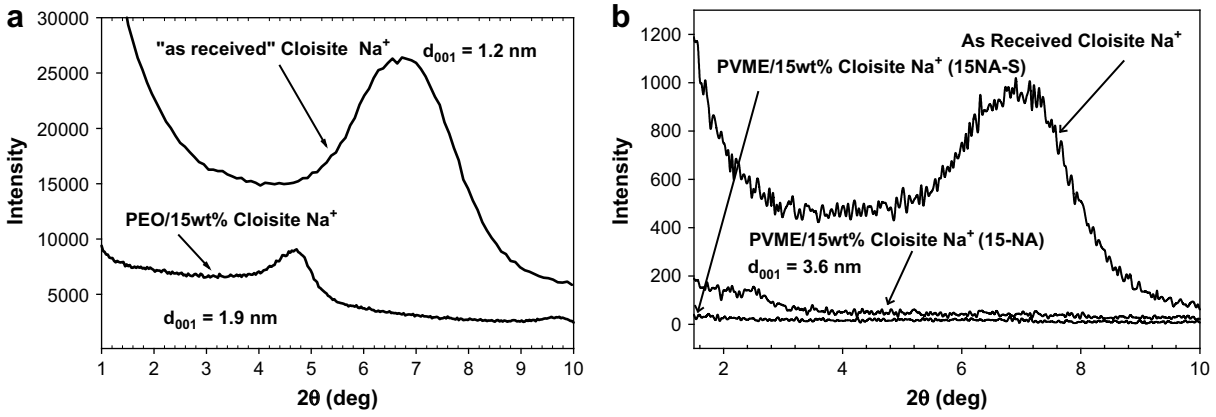

Fig. 2. (a) WAXD of sample Cloisite Na^+/PEO reveals the sample is intercalated as evident by the significant shifting of the d_{001} diffraction peak and the presence of higher order peaks (d_{002}).(b) WAXD of PVME/Na^+ samples 15-NA, 15NA-S, and as received Cloisite Na^+. Sample 15-NA has a weak diffraction peak thought to be the result of a disordered intercalated structure and sample 15NA-S is delaminated as evident by the lack of a coherent diffraction pattern.

Na^+/PVME samples as "weakly interacting" as a basis of comparing them to other organically modified clay/PVME samples which can exhibit other more favorable interactions.

3.2.2. PVME – highly dispersed versus $scCO_2$-processed

A key difference between the *$scCO_2$ processed* samples and the freeze dried sample is the absence of a coherent diffraction peak for freeze-dried sample 15NA-S. The lack of a d_{001} diffraction peak in this sample is indicative of a "highly dispersed" nanocomposite. This is expected because Cloisite Na^+ swells and dissociates in water. The presence of the polymer in a viscous water solution, and the subsequent lyophilization would be expected to reduce the re-aggregation of some of the clay platelets that is usually seen in solution blending. Although a disappearance of the peak in XRD does not alone indicate exfoliation, the clay loading in the sample is high enough (3 times higher than that needed to produce a coherent diffraction peak) to ensure that WAXD provides an adequate representation of the clay morphology. Morgan et al. showed at silicate loadings of less than 5 wt%, coherent diffraction patterns were not always present [38]. The absence of a diffraction peak was further corroborated by additional measurements on different regions of the sample which readily superposed onto the reported diffraction data. Therefore, we fully expect that sample 15NA-S is a highly dispersed nanocomposite. It is worth noting that WAXD data collected from different regions of the intercalated Cloisite Na^+ based nanocomposite (15-NA) and other similar samples, not otherwise discussed in this paper, always resulted in a small but perceivable diffraction peak. This suggests that at these filler loadings it is unlikely that a significant decrease in parallel registry alone could account for the lack of a diffraction peak from sample 15NA-S but rather the platelets are separated beyond the small angle limit of WAXD.

Linear viscoelastic measurements of the *intercalated* "weakly-interacting" $scCO_2$-processed nanocomposite (sample 15-NA) show a 100% increase in G′ near the plateau region and the terminal region (Fig. 3a). The frequency dependence of the dynamic moduli is similar to that of pure PVME. The crossover frequency (Fig. 3c) of the intercalated $scCO_2$-processed sample is factor of 2 lower than that of pure PVME. Even though this is a filled system, with a spectrum of relaxation times, the small change in the matrix chain crossover frequency suggests that the chain relaxation may not have been significant altered by the clay. This could be a consequence of weaker polymer–clay interaction and relatively poor dispersion.

Conversely, the frequency dependence of the highly dispersed "weakly interacting" nanocomposite (sample 15NA-S) is distinctly different from that of the host matrix (Fig. 3b). The dynamic moduli for the highly dispersed nanocomposite do not exhibit terminal relaxation behavior like the host matrix or the intercalated nanocomposite. G′ and G″ are more than an order of magnitude higher, at low frequencies, than the neat matrix. The 15NA-S nanocomposites exhibits non-terminal behavior with $G' \propto \omega^{0.8}$ and $G'' \propto \omega^{0.7}$ rather than $G' \propto \omega^2$ and $G'' \propto \omega$ which may be due to the pseudo-solid network form by the presence of the dispersed nanoclay. The cross-over frequency for the highly dispersed nanocomposite is also significantly decreased relative to the host matrix (~factor of 7). When looking at a log–log plot of the dynamic moduli vs. frequency, the G′ and G″ curves of the partially exfoliated "weakly-interacting" hybrid display an extended region where their values are very close, which makes it difficult to see the cross-over frequency. In order to clarify the cross-over frequency shifts, the dynamic moduli for the neat polymer and the hybrids are plotted on a log–linear graph, which clearly reveals the cross-over points of the two nanocomposites relative to the neat PVME. The temperature dependence of the frequency shift factors (a_T) for intercalated "weakly-interacting" and partially exfoliated "weakly-interacting" hybrids appear unaltered by the silicate loading and the degree of dispersion suggesting that the temperature dependent segmental relaxation dynamics are unaffected by the presence of the silicate (shift factor plots can be seen as inlays in the plots of dynamic moduli). This behavior has been well documented for many nanocomposites and is attributed to the small percentage of polymer chains that are constrained by the silicate surface [27]. Interestingly, the global relaxation dynamics of the polymer chains appear to be sensitive to the degree of silicate dispersion as noted by the significant change in characteristic relaxation time ($\sim 2\pi/\omega_x$) of the nanocomposites relative to the polymer. The characteristic relaxation time of the intercalated nanocomposite is ~16 s compared with ~8 s for the neat polymer matrix. The partially exfoliated nanocomposite has a characteristic relaxation time of ~52 s. Chain dynamics of polymer confined by dispersed nano-clay platelets may deviate significantly from that in their one-component melt. Polymer–clay and clay–clay interaction add further complexity by introducing multi-scale relaxation processes. For example, when clay dispersion is significant, there can be appreciable interaction between the clay and the polymer, thereby contribution slower relaxation modes, which lower the 'overall' terminal relaxation times. In contrast, when there is poor dispersion, the polymer–clay contacts are diminished, with the matrix polymer relaxation mainly unaltered. In our system, the differences in the cross-over frequency may provide insights into the degree of

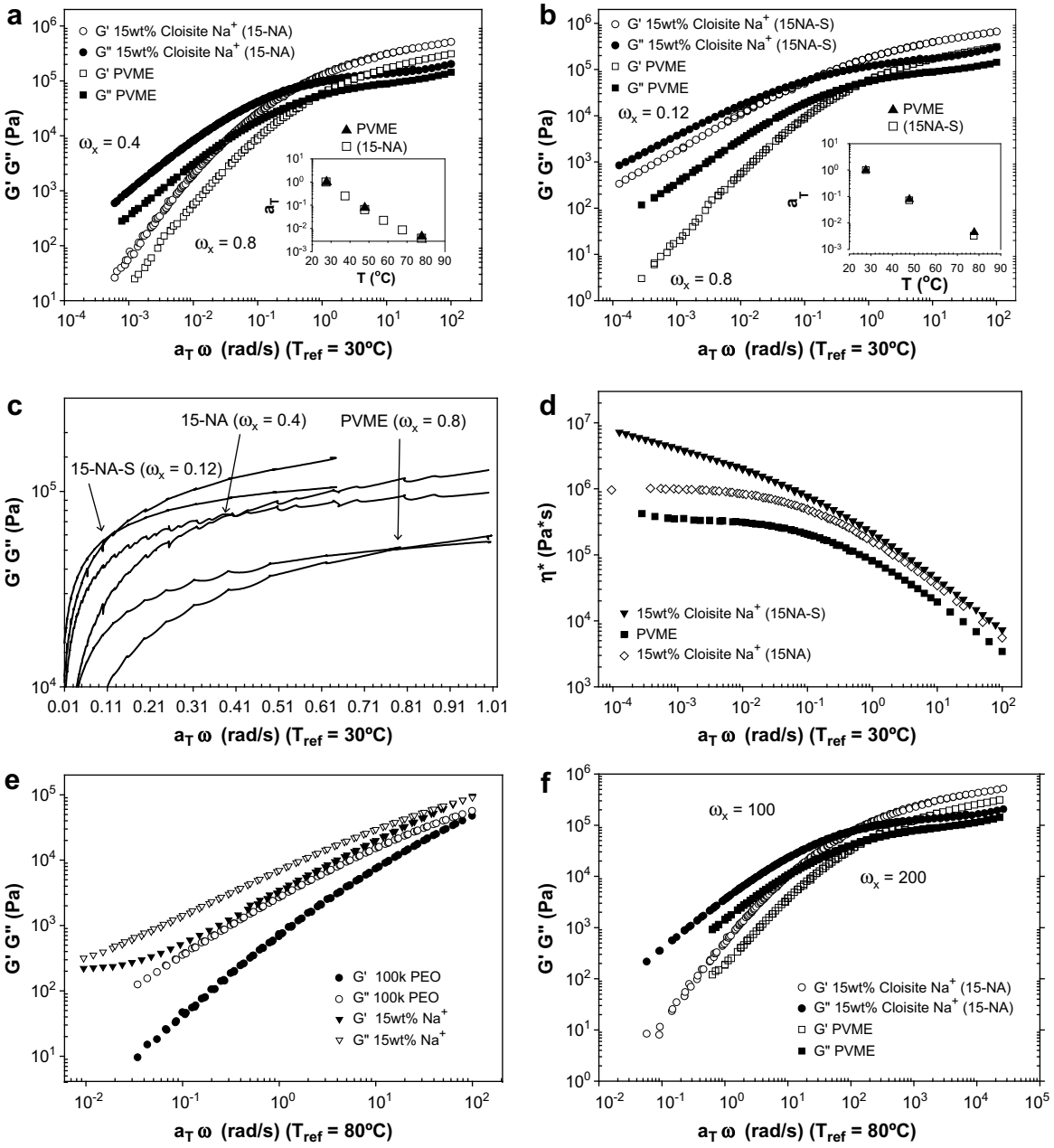

Fig. 3. (a) Log–log plot of dynamic moduli vs. reduced frequency for sample 15-NA (frequency shift factors shown as inlays). Interestingly, there is a factor of 2 decrease in the cross-over frequency suggesting that the global chain dynamics have been altered by the presence of the nano-clay.(b) Log–log plot of dynamic moduli vs. reduced frequency for sample 15NA-S (frequency shift factors shown as an inlay). This sample demonstrates substantially non-terminal relaxation behavior below the cross-over frequency with G′ $\propto \omega^{0.8}$ and G″ $\propto \omega^{0.7}$. In addition, the cross-over frequency is shifted by ~a factor of 6.5.(c) Log–linear plot of dynamic moduli vs. reduced frequency to more clearly show the cross-over frequency of the neat PVME and the hybrids.(d) Complex viscosity of the neat PVME and both hybrids. e) Log–log plot of dynamic moduli vs. reduced frequency for 15 wt% Cloisite Na^+/PEO nanocomposite with a reference temperature of 80 °C.(f) Log–log plot of dynamic moduli vs. reduced frequency for 15 wt% Cloisite Na^+/PVME nanocomposite with a reference temperature of 80 °C for comparison with the PEO nanocomposites.

silicate dispersion. The cross-over frequency of the partially exfoliated nanocomposite is much lower than that of the intercalated nanocomposite, most likely the result of higher exposed surface area in the case of the partially exfoliated sample, slowing down the 'mean terminal relaxation' of the polymer chains.

In addition to changes in G′ and G″, the complex viscosity also exhibits significantly different behavior as a function of dispersion (Fig. 3d). The intercalated sample (15-NA) has ~150% increase in "complex" zero-shear viscosity and displays Newtonian-like behavior at low frequencies like the neat polymer. At the lowest frequencies measured, the highly dispersed sample (15NA-S) has ~1000% increase in viscosity relative to the host matrix and exhibits shear thinning behavior at all shear rates measured. Although, G′ and G″ of the highly dispersed sample never becomes independent of frequency, and the zero-shear viscosity does not diverge, it is clear that dispersion still plays a key role in the viscoelastic response of "weakly-interacting" polymer silicate nanocomposites.

3.3. Role of polymer–clay interactions with comparable levels of intercalation

In the previous section we described the impact of nano -clay dispersion on the melt rheological properties of nanocomposites

when *"weakly-interacting"* PVME–clay nanocomposites are *either 'highly dispersed' or 'intercalated'*. Here we discuss the *role of polymer–clay interactions* on the viscoelastic response of a series of PVME organo-clay nanocomposites using three *intercalated* organophilic clay/PVME nanocomposites prepared via *scCO$_2$ processing* [Cloisite 30B (sample 15-30B), and I.30P (sample 15-I.30P)]. The extent of polymer–clay interactions could vary with each of the organically modified clays. Cloisite 30B is expected to form hydrogen bonds with PVME. All the nanocomposites discussed in this section were made via the *scCO$_2$ process* and as a result of the selected processing conditions are intercalated.

The presence of hydrogen bonds in sample 15-30B was studied using FTIR spectroscopy (Fig. 4: IR spectroscopy of Cloisite 30B shows a small OH stretching peak at 3650 cm^{-1}. No OH stretching peak is present in the pure PVME or clay). The nanocomposite displays two distinct peaks in the region for OH stretching, the one at 3650 cm^{-1} are free hydroxyl groups and the peak at 3350 cm^{-1} are hydroxyl groups which have formed weak hydrogen bonds with the PVME (Fig. 4c). The proposed hydrogen bond may be between the surfactant and the PVME (Fig. 4d) not directly with the surface of the nano-clay as is the case with polyamide-6 nanocomposites. The hydrogen bonds are considered weak because the shift in wave number relative to the wave number of the free hydroxyl group is less than 500 cm^{-1}. The FTIR spectra of the other polymer–clay systems did not show the presence of any additional peaks other than these from PVME and clay. It is difficult to quantify hydrogen bonding interactions in these complex systems. The detailed characterization is beyond the scope of the manuscript. We suggest that the difference in the FTIR spectral signatures between the different clays, may be indicative of hydrogen bonding, as used before by others [39,40].

The inter-gallery spacing of I.30P (sample 15-I.30P) and Cloisite 30B (sample 15-30B) in PVME was determined to be 2.7 and 2.4 nm respectively (Fig. 5). These inter-gallery spaces represent an increase of 1.2 nm for I.30P and 1.55 nm for Cloisite 30B. This increasing in spacing may be a strong indication that polymer has penetrated the space between the clay platelets. In addition to a decrease in the Bragg angle, indicated by the increase in the basal spacing, diffraction patterns from the nanocomposites formed from the organically modified clays (samples 15-30B, and 15-I.30P) exhibited changes in peak profile compared with the as-received clay. Specifically, the peak breadth at full-width half maximum "B" decreased in the nanocomposites relative to their corresponding "as-received" nano-clay. The decrease in peak breadth is expected with intercalated nano-clays because the clay galleries expand, resulting in an increase in the overall tactoid size (height). Previous research shows that small crystal sizes give broad diffraction patterns and larger crystals have narrower patterns [39]. The shape and width of the diffraction patterns were analyzed to provide a rough approximation of the tactoid size. Because the diffraction patterns produced by the organo-philic nanocomposites were Gaussian in nature we employed the Scherrer Equation to determine the average tactoid thickness.

$$t := \frac{\lambda}{B\cos\theta_B}$$

From the average tactoid thickness we determined the average number of platelets per tactoid using the following equation:

$$\eta := \frac{t - 10}{d_{001}} + 1$$

Where t is the tactoid thickness determined from the Scherrer equation, 10 is the thickness of a platelet in angstroms, d_{001} is the basal spacing of the nano-clay, and η is the number of platelets rounded to the next integer (see justification in Appendix). The Scherrer equation predicted the minimum average number of platelets per tactoid as 3–5 for the Na^+ nanocomposites (Table 2). The values obtained from the Scherrer equation are underestimated since the correction for equipment broadening is not used in the calculations. Also, the shape of the clay particles is not truly spherical and the Scherrer equation can only provided a rough estimate of the tactoid size. The presence of 3 diffraction peaks in some of the samples further supports the existence of larger structures because tens of plates are needed to obtain well defined higher order diffraction patterns [41]. The values calculated via the Scherrer equation agree well with literature [27].

Even though the WAXD measured *d*-spacing in I.30P and 30B intercalated nanocomposites are somewhat similar they have the same volume fraction of inorganic nano-clay (4 vol%) which is important when comparing the viscoelastic properties of nanocomposites, rheology shows significant difference. The dynamic moduli for the samples are compared in three regions: below the cross-over frequency (terminal region), above the cross-over frequency (plateau region), and at the cross-over frequency.

3.3.1. PVME-30B nanocomposite

G′ of the hydrogen bonded nanocomposite (sample 15-30B) was increased by 150% in the plateau region and more than an order of magnitude in the terminal region (Fig. 6a). At low frequencies, sample 15-30B displays distinctly non-terminal behavior with G′ $\propto \omega^{0.5}$ and G″ $\propto \omega^{0.7}$. This non-terminal behavior is also apparent in the complex viscosity, which exhibits shear thinning behavior over the entire frequency range with a trend toward diverging viscosity at the lowest shear rates measured (Fig. 6b). The cross-over frequency of sample 15-30B is reduced by ~a factor of 4 relative to the host matrix. To verify that the change in cross-over frequency was indeed the result of changes in relaxation time and not a manifestation of time temperature superposition, the frequency shift factors of the nanocomposite and the neat matrix were compared. The frequency shift factors for the nanocomposite are nearly identical to that of pure PVME. This suggests that local (segmental) chain dynamics of the intercalated nanocomposite are unaltered, at least within the sensitivity of the measurement and that the polymer chains do not form hydrogen bonds directly with the silicate surface as is the case in many polyamide-6 nanocomposites [42]. Furthermore, it shows that the global chain dynamics have been impacted by the presence of the nano-clay in the PVME.

3.3.2. PVME-I.30P nanocomposite

The storage modulus of scCO$_2$ processed 15-I.30P sample increases by ~100% in the plateau region. Furthermore, 15-I.30P exhibits no terminal behavior (G′ $\propto \omega^{0.5}$ and G″ $\propto \omega^{0.6}$) and is nearly 2 orders of magnitude larger than the neat PVME in the terminal region (Fig. 6c). The cross-over frequency shifts by an order of magnitude relative to the neat PVME and the characteristic relaxation time increases from ~8 s to ~78 s. The frequency shift factors for sample 15-I.30P are nearly identical to the neat polymer suggesting that the change in cross-over frequency was indeed the result of changes in relaxation time. The pseudo solid-like behavior seen in G′ of sample 15-I.30P is also observed in the complex viscosity at low shear rates where the viscosity diverges with shear thinning behavior prevalent thought the whole frequency spectrum (Fig. 6d). The cross-over frequency shift of sample 15-I.30P is much greater than that of sample 15-NA, suggesting that the relaxation dynamics of the polymer chain may be significantly impacted by the strength of the polymer–clay interactions. In addition, longer relaxation events are also affected by the strength

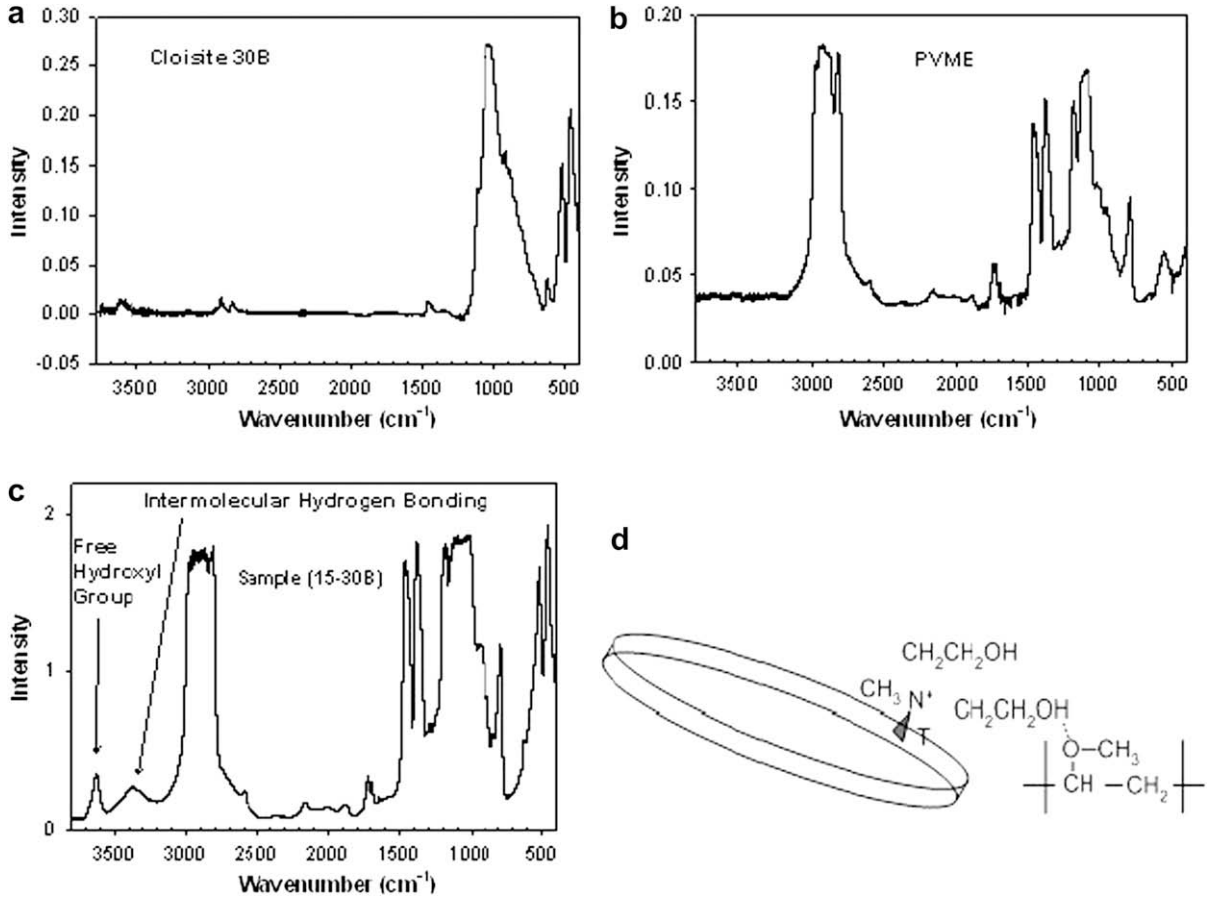

Fig. 4. (a) FTIR spectroscopy of Cloisite 30B shows free hydroxyl group stretch (peak 3650 cm^{-1}).(b) FTIR spectroscopy of PVME shows the absence of an intermolecular hydrogen bond peak (3350 cm^{-1}).(c) FTIR spectroscopy of sample 15-30B has an intermolecular hydrogen bond peak (3350 cm^{-1}).(d) Proposed hydrogen bond between surfactant and PVME.

of the polymer–clay interactions as evident by the non-terminal behavior in sample 15-I.30P and the terminal behavior seen in sample 15-NA.

Samples 15-30B and 15-I.30P displayed qualitatively similar rheological behavior with 15-I.30P nanocomposite showing more low-frequency enhancement than that of sample 15-30B. The viscosity of sample 15-I.30P increases by ~2 orders of magnitude and that of sample 15-30B increases by ~1.5 orders of magnitude. The extent of intercalation is expected to be similar between these samples because the inter-gallery spacing is similar in each of the nano-clays with both reaching a new equilibrium spacing within 20% of each other. Therefore, both samples are expected to be highly intercalated. The reason for the large disparity in cross-over frequencies of the two samples is not clear. This may be the result of a slightly higher degree of intercalation in sample 15-I.30P but is more likely the result of how the polymer interacts with the clay. Nanocor I.30P has an average higher aspect ratio of 350 (Nanocor) while Cloisite 30B has an average aspect ratio of 110 (Southern Clay

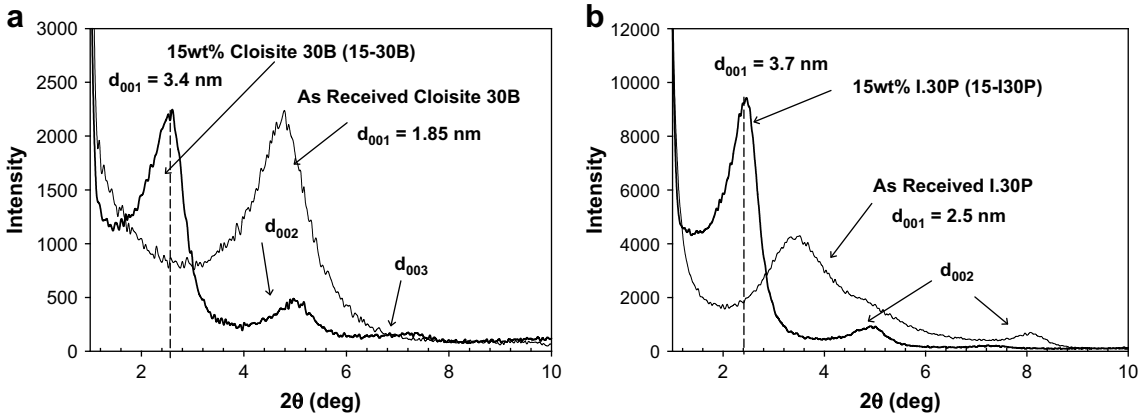

Fig. 5. (a) WAXD of sample 15-30B reveals the sample is intercalated as evident by the significant shifting of the d_{001} diffraction peak and the presence of higher order peaks (d_{002} and d_{003}).(b). WAXD of sample 15-I.30P reveals that the sample is intercalated.

Table 2
The first entry in each column refers to the nanocomposite and the second, in parenthesis, refers to the as-received nano-clay corresponding to a particular nanocomposite. n/a appears where no diffraction pattern was observed or the pattern did not resemble a Gaussian distribution.

Name	B (rad)	d_{001} (nm)	# Platelets/tactoid	$2\theta_B$ (deg)
15-30B (30B)	0.022 (0.025)	3.4 (1.85)	3 (4)	2.59 (4.78)
15-NA (Na^+)	n/a	3.6 (1.2)	n/a	2.45 (7.1)
15-I.30P (I.30P)	0.011 (0.034)	3.7 (2.5)	5 (3)	2.5 (3.5)
15NA-S (Na^+)	n/a	n/a (1.2)	n/a	n/a (7.1)
Cloisite Na+/PEO	0.024 (0.035)	1.9 (1.2)	3 (3)	4.69 (7.1)

Products). With 4 vol% and 350 average aspect ratio, Nanocor I.30P nanocomposite there are ~416 platelets/μm^3 which leads to a maximum nano-clay surface area of ~81 m^2/cm^3 of nanocomposite. In the case of Cloisite 30B the 4 vol% and 110 average aspect ratio there are ~4346 platelets/μm^3 which leads to a maximum nano-clay surface area of ~84 m^2/cm^3 of nanocomposite. The viscoelastic response depends strongly on the volume fraction of inorganic platelets, the dispersion state, and the level of interactions between polymer and clay and also between the clay platelets themselves. The clay platelets interaction is in the form of clay platelet edge-to-face interactions and it results in the formation of a so-called "house of cards" structure, which is generally recognized to be the primarily culprit for the increase in G′ at low shear rates (the structure breaks up at higher shear rates). However since both samples contains the same volume fraction of inorganic matte, we believe that the clay–clay interaction should not play a big role in the rheological differences between the two nanocomposites. Both samples have the same volume fraction of inorganic nano-clay and similar maximum surface areas available for polymer–clay interactions; however the Nanocor I.30P nanocomposite shows improved rheological properties compared to Cloisite 30B nanocomposites. This suggests that PVME can interact with and coat Nanocor I30P to a greater extent compared to Cloisite 30B, which we believe may be responsible for the differences in the viscoelastic properties between 15-I.30P and 15-30B. Also, since the I.30P average aspect ratio is higher than 30B could be another explanation of why 15-I.30P nanocomposite shows improvements in viscoelastic properties over 15-30B nanocomposite. Higher aspect ratio platelet results in a more effective load transfer and is observed to give greater increases in G′. This phenomenon was also observed in fiber composites if the critical fiber length in short [43]. Sample 15-30B still displays significant improvement in viscoelastic properties over the polymer matrix which suggests that hydrogen bonding between the ammonium salt and the PVME (Fig. 4d) may play role in the overall viscoelastic response of sample 15-30B. Comparison of samples 15-I.30P and 15-30B with sample 15-NA, strongly suggests that the extent of interaction between the clay and the polymer plays a key role in the linear viscoelastic response of these nanocomposites. Another plausible explanation for the differences in the viscoelastic response between these system is that 15-NA contains slightly higher volume of inorganic mater (5 vol%) compared to 15-30B and 15-I.30P (4 vol%) which can increase the parallel stacking of the layers and/or agglomerate

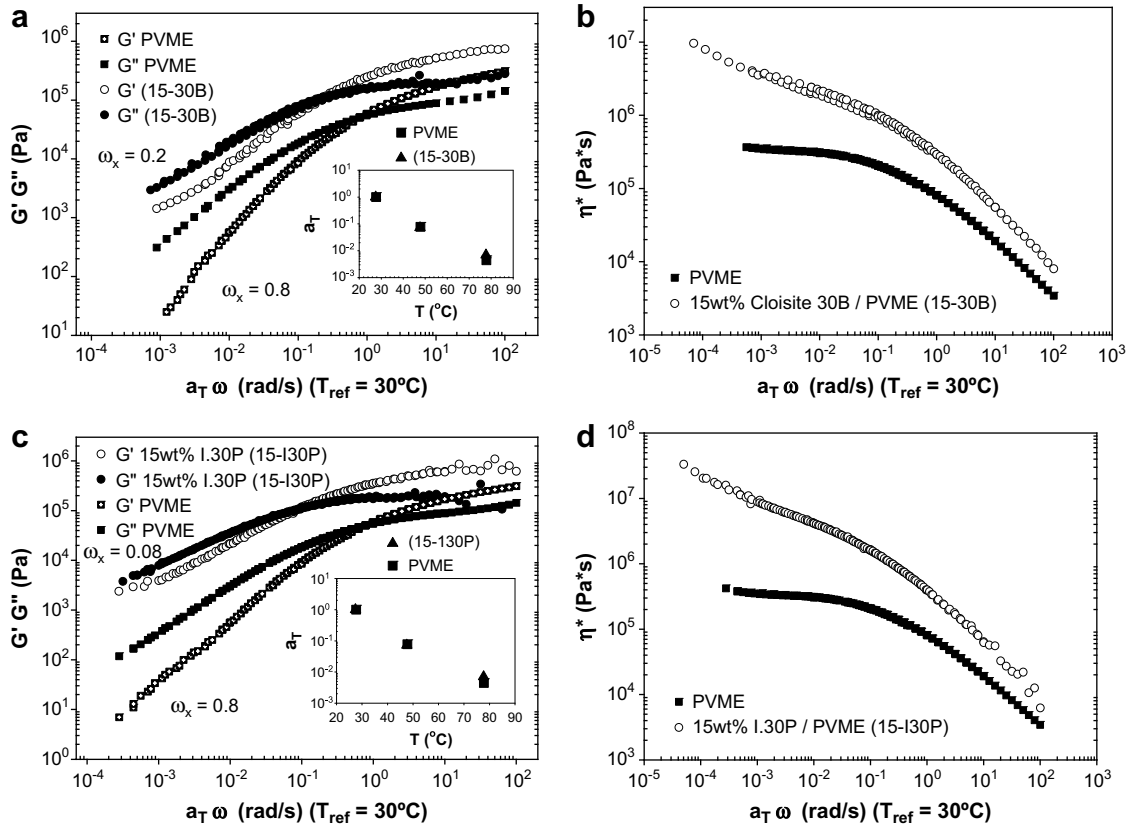

Fig. 6. (a) Log–log plot of dynamic moduli vs. reduced frequency for sample 15-30B (frequency shift factors shown as an inlay). The moduli display distinctly non-terminal behavior and a factor of 4 decrease in the cross-over frequency of the nanocomposite relative to the neat polymer.(b) Complex viscosity vs. reduced frequency for sample 15-30B diverges at low frequencies. c) Log–log plot of dynamic moduli vs. reduced frequency for sample 15-I.30P (frequency shift factors shown as an inlay). The moduli display distinctly non-terminal behavior and there is an order of magnitude decrease in the cross-over frequency of the nanocomposite relative to the neat polymer.(d) Complex viscosity vs. reduced frequency for sample 15-I.30P displays a diverging viscosity at low frequencies.

formation. The increase in the parallel stacking disfavor edge-to-face interactions because there is physically no room for such interactions to occur and more faces become inaccessible to the layer edges. This, in turn, would be expected to suppress the formation of a strongly interacting filler network, which can be a plausible explanation for the less improvement in G′ in the (higher inorganic content) Na^+ system vs. the (lower inorganic content) 30B and I.30P systems. However, the differences in volume loading of inorganic matter are small and we believe that it doesn't impact the rheological response to a great extent. Furthermore, Cloisite Na^+ contains no organic modifier while 30B and I.30B both do and the interactions between PVME and the organically modified clay are expected to be stronger then PVME-Na^+ interactions. Previously, Shi et al. demonstrated that interactions between the alkyl chains of the ammonium salt and the polymer matrix were weak and had a small impact on the reinforcement properties (tensile strength) of the nanocomposite relative to the host matrix. They concluded that polymer chains binding (adsorbed) directly to the clay surface were responsible for the majority of the enhancements [44]. Therefore, it appears that the adsorption of PVME onto the clay surface is at least partially governed by the type of organic modifier present and that the modifier may significantly improve the adsorption.

4. Conclusions

We investigated the impact of nano-clay dispersion and polymer–clay interaction on the viscoelastic response of PVME/clay and PEO/clay nanocomposites with varying degrees of dispersion and polymer–clay interactions. The use of water-soluble PVME and water-soluble natural clay provided a benchmark for a highly dispersed sample. The use of $scCO_2$ processing produced intercalated nanocomposites with somewhat similar final WAXD patterns, yet the rheological properties were significantly different. Even though the extent and the nature of dispersion and interactions in theses complex systems are tough to quantify, rheology offers valuable insights into the mesoscale structure and interactions. The viscoelastic response of polymer–clay nanocomposites is sensitive to the extent of dispersion and the degree of interaction. Comparison of $scCO_2$-processed (intercalated) and water-processed (highly dispersed) Cloisite Na^+/PVME nanocomposites with "weak polymer–filler interactions" (suggested that high level clay dispersion results in non-terminal behavior ($G' \propto \omega^{0.8}$ and $G'' \propto \omega^{0.7}$) and a factor of 8 decrease in the cross-over frequency, and an order of magnitude increase in the low-frequency storage moduli; while intercalation results in a filler effect with the relaxation behavior of the bulk polymer virtually unaltered by the presence of the nano-clay. In contrast, for intercalated systems with "stronger" polymer–clay interactions (PVME/I.30P), there is a low-frequency plateau, an order of magnitude decrease in the crossover frequency, and more than two orders of magnitude increase in low-frequency storage moduli. Furthermore, PVME/I.30P sample displays enhanced rheological properties compared to PVME/30B sample despite having similar dispersion, same inorganic volume fraction and same maximum surface area indicating the presence of stronger polymer–clay interactions. These results suggest that rheology can offer valuable insights into these complex systems. When 'strong' polymer–clay interactions are present, even an intercalated structure can produce significant property improvements (even more than highly dispersed systems). Hence, the combination of WAXD and rheology can provide insights into the extent of dispersion and compatibility of the nano-clay with the chosen polymer matrix.

Acknowledgements

Funding from NSF (CTS 0335315), WSU-Institute of Manufacturing Research (GRA-SH and MM), and nanoSEC (NSF SBIR Phase II 0646447 subcontract) are greatly appreciated.

Appendix

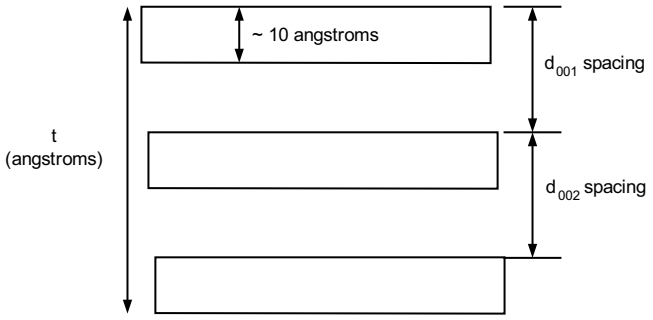

$$t = d_{001} \times (n-1) + 10$$

From the drawing it can be seen that the thickness of a tactoid can be represented by the equation above where $(n-1)$ is the number of clay platelets in the tactoid minus 1 and is equal to the number of inter-gallery spacing that needs to be accounted for. Multiplying $(n-1)$ with the d_{001} spacing gives the height of the stack shy the thickness of one plate. The 10 on the right hand side of the equation, at the end, represents that plate thickness and has units of angstroms. The Scherrer equation can be used to determine the thickness "t" from the FWHM value of the d_{001} diffraction peak. From there, the equation above is solved for n.

References

[1] Giannelis EP. Advanced Materials (Weinheim, Germany) 1996;8(1):29–35.
[2] Giannelis EP. Applied Organometallic Chemistry 1998;12(10/11):675–80.
[3] Giannelis EP, Krishnamoorti R, Manias E. Advances in Polymer Science 1999;138:107–47. Polymers in Confined Environments.
[4] Gilman JW. Applied Clay Science 1999;15(1–2):31–49.
[5] Gilman JW, Jackson CL, Morgan AB, Harris Jr R, Manias E, Giannelis EP, et al. Chemistry of Materials 2000;12(7):1866–73.
[6] Kojima Y, Usuki A, Kawasumi M, Okada A, Kurauchi T, Kamigaito O. Journal of Polymer Science, Part A: Polymer Chemistry 1993;31(4):983–6.
[7] Messersmith PB, Giannelis EP. Journal of Polymer Science, Part A: Polymer Chemistry 1995;33(7):1047–57.
[8] Ren J, Casanueva BF, Mitchell CA, Krishnamoorti R. Macromolecules 2003;36(11):4188–94.
[9] Usuki A, Kojima Y, Kawasumi M, Okada A, Fukushima Y, Kurauchi T, et al. Journal of Materials Research 1993;8(5):1179–84.
[10] Vaia RA, Price G, Ruth PN, Nguyen HT, Lichtenhan J. Applied Clay Science 1999;15(1–2):67–92.
[11] Zhu J, Morgan AB, Lamelas FJ, Wilkie CA. Chemistry of Materials 2001;13(10):3774–80.
[12] Blumstein A. Journal of Polymer Science, Part A: General Papers 1965;3(7):2653–64.
[13] Aranda P, Ruiz-Hitzky E. Chemistry of Materials 1992;4(6):1395–403.
[14] Burnside SD, Giannelis EP. Chemistry of Materials 1995;7(9):1597–600.
[15] Fornes TD, Yoon PJ, Keskkula H, Paul DR. Polymer 2001;42(25):09929–40.
[16] Lepoittevin B, Pantoustier N, Devalckenaere M, Alexandre M, Kubies D, Calberg C, et al. Macromolecules 2002;35(22):8385–90.
[17] Ray SS, Okamoto M. Progress in Polymer Science 2003;28(11):1539–641.
[18] Vaia RA, Giannelis EP. Macromolecules 1997;30(25):8000–9.
[19] Vaia RA, Ishii H, Giannelis EP. Chemistry of Materials 1993;5(12):1694–6.
[20] Vaia RA, Jandt KD, Kramer EJ, Giannelis EP. Macromolecules 1995;28(24):8080–5.
[21] Weimer MW, Chen H, Giannelis EP, Sogah DY. Journal of the American Chemical Society 1999;121(7):1615–6.
[22] Xu L, Reeder S, Thopasridharan M, Ren J, Shipp DA, Krishnamoorti R. Nanotechnology 2005;16(7):514–21.
[23] Hoffmann B, Kressler J, Stoppelmann G, Friedrich C, Kim GM. Colloid and Polymer Science 2000;278(7):629–36.
[24] Krishnamoorti R, Giannelis EP. Macromolecules 1997;30(14):4097–102.

[25] Krishnamoorti R, Ren J, Silva AS. Journal of Chemical Physics 2001;114(11): 4968–73.
[26] Krishnamoorti R, Yurekli K. Current Opinion in Colloid & Interface Science 2001;6(5,6):464–70.
[27] Ren J, Silva AS, Krishnamoorti R. Macromolecules 2000;33:3739–46.
[28] Horsch S, Serhatkulu G, Gulari E, Kannan RM. Polymer 2006;47(21):7485–96.
[29] Manitiu M, Bellair RJ, Horsch S, Gulari E, Kannan RM. Macromolecules 2008;41:8038–46.
[30] Horsch S, Serhatkulu G, Gulari E, and Kannan RM. Unpublished data.
[31] Fetters LJ, DJLaRH Colby. Chain dimensions and entanglement spacings physical properties of polymers handbook. New York: Springer; 2007. p. 447–54.
[32] Manke CW, Gulari E, Mielewski DF, and Lee EC. System and method of delaminating a layered silicate material by supercritical fluid treatment. US Patent 6,469,073, October 2002.
[33] Mielewski DF, Lee EC, Manke CW, and Gulari E. System and method of preparing a reinforced polymer by supercritical fluid treatment. vol US Patent 6,753,360 US Patent 6,753,360, June 2004.
[34] Gulari E, Serhatkulu GK, and Kannan R. Method of delaminating aggregated particles with a coating agent in a supercritical fluid. vol. US Patent Application 20,050,014,867. US Patent Application 20,050,187,330, February 2004.
[35] Gulari E and Serhatkulu GK. Method of delaminating a graphite structure with a coating agent in a supercritical fluid. US Patent Application 20,050,014,867, July 2003.
[36] Pandey RB, Farmer BL. Journal of Polymer Science, Part B: Polymer Physics 2008;46:2696.
[37] Strawhecker KE, Manias E. Chem Mater 2003;15:844–9.
[38] Morgan AB, Gilman JW. Journal of Applied Polymer Science 2003;87(8):1329–38.
[39] Cullity BD, Stock SR. Elements of X-ray diffraction. 3rd ed. Pearson Education; 2001.
[40] Silverstein R, Webster F. Spectrometric identification of organic compounds. 6th ed. John Wiley & Sons, Inc.; 1998.
[41] Brindley G, Brown G. Crystal structures of clay minerals and their X-ray identification. London: Mineralogical Society; 1980.
[42] Kojima Y, Usuki A, Kawasumi M, Okada A, Kurauchi T, Kamigaito O. Journal of Polymer Science, Part A: Polymer Chemistry 1993;31(7):1755.
[43] Kardos JL. Pure & Applied Chemistry 1985;57(11):1651–7.
[44] Shi H, Lan T, Pinnavaia TJ. Chemistry of Materials 1996;8(8):1584–7.